RAPID COMMUNICATIONS

PHYSICAL REVIEW B VOLUME 44, NUMBER 4 15 JULY 1991-II

Valence-band coupling in thin (Ga,In)As-AlAs strained quantum wells

Bernard Gil, Pierre Lefebvre, and Philippe Boring
Groupe d'Etudes des Semiconducteurs, Université de Montpellier II: Sciences et Techniques du Languedoc, Case Courrier 074, 34095 Montpellier CEDEX 5, France

Karen J. Moore, Geoffrey Duggan, and Karl Woodbridge
Philips Research Laboratories, Redhill, Surrey RH1 5HA, England
(Received 22 April 1991)

Model representations of varying complexity are used to describe the band structure of semiconductor quantum wells and superlattices. However, the physics of valence-band-confined states is usually restricted to the upper Γ_8^v band. We report spectroscopic measurements of the light- to heavy-hole splitting in (Ga,In)As-AlAs strained multiple quantum wells. The results are compared to two types of theoretical calculations: (i) within the framework of the usual approximations, and (ii) taking account of the Γ_7^v split-off states, which are mixed with the light-hole ones. We demonstrate the crucial influence of the valence-band coupling, by a significant improvement of the agreement between theory and experiments. Competitive effects of thicknesses, potential-well depths, and magnitude of the Γ_8^v-Γ_7^v splitting are detailed and discussed.

The advent of low-dimensional systems such as quantum wells or superlattices has revolutionized solid-state electronics. The possibility of achieving the coherent growth of various semiconductor compounds on low-cost substrates opens up opportunities for devices with new potential applications. A tremendous activity has developed in order to correlate the physical properties of these structures to their design. The physics of these artificial semiconductors is derived from the bulk properties, but the reduction of dimensionality gives rise to alternate properties: Fundamental phenomena such as the quantum Hall effect and fractional quantum Hall effect[1] are typical of two-dimensional semiconductors. Also, the possibility of tuning the miniband width of superlattices produces the Wannier-Stark localization[2] under moderate electric-field conditions, while this effect cannot be observed in the bulk. Another growing area of interest in the physics of low-dimensional systems concerns strained-layer semiconductors where the different layers which constitute the microstructure are lattice mismatched with each other, and sometimes with the substrate.[3] Coherent growth is impossible to achieve beyond a critical thickness[4] where dislocations are generated, with disastrous consequences on the basic characteristics of the materials: collapse of the mobilities,[5] quenching of the radiative lifetimes, etc. Beneath the critical thickness, the layers experience a built-in elastic strain field which lowers their lattice symmetry. The modifications of the electronic levels in the deformed layers can quantitatively be correlated to the strain via a set of phenomenological quantities: the deformation potentials. This paper reports on the (Ga,In)As-AlAs combination, where both layers are elastically strained so as to match their in-plane lattice parameter to the lattice parameter of the GaAs substrate.[6] We have varied the thicknesses of the (Ga,In)As confining layers in order to observe experimentally the coupling of the light-hole states with the split-off band. This effect, which can be predicted from group theory arguments,[7,8] is unambiguously observed and quantified. The paper is organized as follows: The experimental results are described in the next section, then we outline the formalism used to calculate the electronic structure of our samples. A theory-experiment comparison is made in the next section, and, finally, we infer some conclusions from our work.

The samples all consist of the same sequence of 20 $Ga_{0.96}In_{0.04}As$ layers sandwiched between 21 AlAs layers. The energy difference between the direct gaps of these materials is ~ 1.6 eV, hence the confining potential wells are deep. The thickness of the AlAs layers is fixed at 4 nm for all the samples, while the thickness of the alloy layers is varied. Samples, hereafter labeled samples 1, 2, 3, 4, correspond to (Ga,In)As thicknesses of 3.8, 3.0, 1.8, and 1.2 nm, respectively. Photoluminescence characterization of these samples has revealed that the band alignment of samples 1 and 2 is type I while samples 3 and 4 have a type-II lineup.[6] Reflectivity has been used in order to measure the energy position of the $e(1)$hh(1) and $e(1)$lh(1) type-I transitions in each sample. Figure 1 summarizes the low-energy reflectance data taken at 2 K. Except for sample 1, one observes a pair of features corresponding to the $e(1)$hh(1) and $e(1)$lh(1) excitons, respectively. Uniaxial stress experiments, which will be detailed elsewhere,[9] have confirmed that the additional features observed for sample 1 correspond to "hot" excitons.[6] As generally observed, the splitting between heavy- and light-hole excitons increases when the thickness of the confining layer diminishes. Envelope function calculations have been performed using the "decoupled subbands approximation," which is generally used to compute the electronic structure of quantum wells at $k_x = k_y = 0$.[10,11] Within this approximation, the eigenfunctions of the quantum-well problem are directly proportional to the Γ_8 Bloch waves $|\frac{3}{2}, \pm\frac{3}{2}\rangle$ and $|\frac{3}{2}, \pm\frac{1}{2}\rangle$, for heavy holes and light holes, respectively.

Applying this simple model to our samples, and allowing a small correction for the binding energy, one adequately calculates the energy of the $e(1)$hh(1) excitons. However, the model always fails to intepret the energy po-

 ©1991 The American Physical Society

sitions of the $e(1)\text{lh}(1)$ features. The discrepancy between the calculation and the observation is most dramatic for thin quantum wells. This is illustrated in Fig. 2, where we have plotted the experimental values of the energy difference between transitions $e(1)\text{lh}(1)$ and $e(1)\text{hh}(1)$ (solid circles) together with the calculated difference of the band-to-band energies (dashed lines). Because the growth parameters are sufficiently well controlled, it is clear that the deviation between the experiment and the calculation originates from the excessive simplicity of the treatment of the valence-band physics in the decoupled subbands approximation.

Writing the 6×6 effective-mass kinetic Hamiltonian at $k_x = k_y = 0$, one sees that it can be represented by two 3×3 block-diagonal matrices corresponding to the subspaces of basis functions $(\phi_h, \phi_l, \phi_{so})$.

$$\phi_h = (X+iY)\alpha/\sqrt{2}\,,\quad \phi_l = [-2Z\alpha + (X+iY)\beta]/\sqrt{6}\,,\quad \phi_{so} = [Z\alpha + (X+iY)\beta]/\sqrt{3}\,, \tag{1}$$

$$H_s + H_{kin} = \begin{array}{c} \\ \end{array}\begin{pmatrix} -(\gamma_1 - 2\gamma_2)k_z^2 & 0 & 0 \\ 0 & -(\gamma_1+2\gamma_2)k_z^2 & 2\sqrt{2}\gamma_2 k_z^2 \\ 0 & 2\sqrt{2}\gamma_2 k_z^2 & -\gamma_1 k_z^2 - \Delta_0 \end{pmatrix}, \quad (|\phi_h\rangle,\ |\phi_l\rangle,\ |\phi_{so}\rangle) \tag{2}$$

where γ_1 and γ_2 are the Luttinger parameters and Δ_0 is the energy of the spin-orbit split-off band. The diagonalization of (2) gives the dispersion relations $E(k_z)$ of the valence-band energies along the [0,0,1] direction, in the absence of stress. In the decoupled subbands approximation, the off-diagonal terms are ignored, and all the bands have a parabolic dispersion. To quantitatively discuss this usually adopted approximation, we have drawn the dispersion relation of the GaAs valence band as a function of k_z, and at $k_x = k_y = 0$. On the left-hand side of Fig. 3, we have plotted the *parabolic* relations obtained when the interaction between the light hole and the split-off hole is ignored. A similar drawing appears in the right-hand side of the figure, but now the interaction is included in the calculation, leading to *nonparabolic* dispersion relations. To make quantitative estimations, we have solved, for both approximations, the infinite well problem for a well width of 5 nm. The light-hole confinement energy is significantly reduced in the coupled subbands approximation (see the solid rectangles in the figure). In fact, the usual limitation of the valence-band states to Bloch states having the Γ_8 symmetry collapses when the depth of the valence-band discontinuity exceeds the value of the Γ_8^v-Γ_7^v energy difference and when the confinement energy of the light hole reaches $\sim\Delta_0/2$ in the decoupled subbands approximation. Now we will treat the real problem of strained layers and finite potential depths.

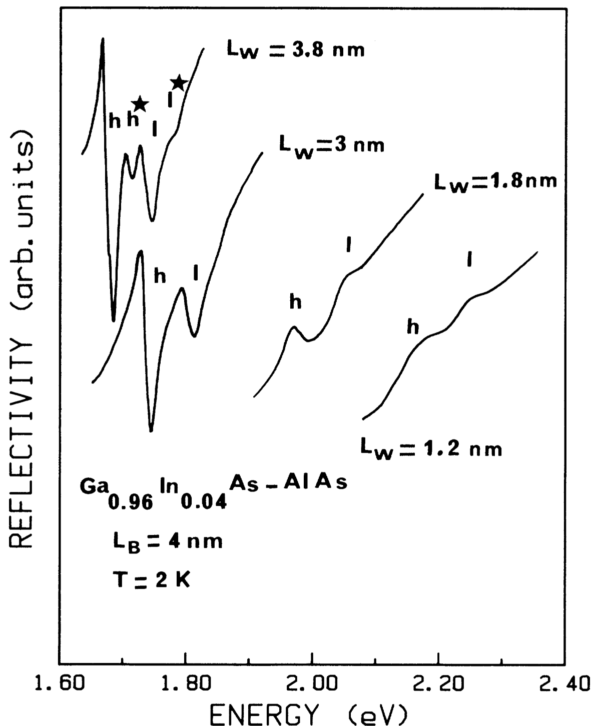

FIG. 1. Reflectance spectra obtained at liquid-helium temperature on four $Ga_{0.96}In_{0.04}As$-AlAs superlattices, having a constant AlAs width of 4 nm. The well thicknesses are indicated on the figure. h and l label the $e(1)\text{hh}(1)$ and $e(1)\text{lh}(1)$ excitonic features in each sample. The transitions labeled h^* and l^* correspond to the creation of hot excitons (see Refs. 6 and 9).

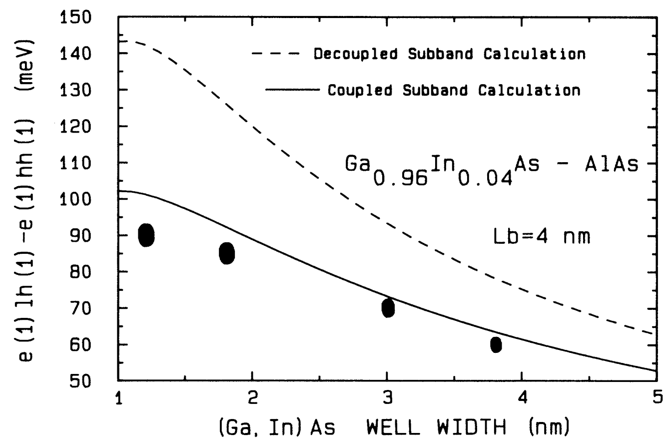

FIG. 2. Comparison of the energy difference between the $e(1)\text{lh}(1)$ and $e(1)\text{hh}(1)$ transitions obtained from experiments (solid circles) and from calculations, for $Ga_{0.96}In_{0.04}As$-AlAs superlattices, with constant barrier width of 4 nm. The dashed curve is obtained when the coupling between light-hole and split-off hole states is neglected, while the solid curve includes this interaction. Excitonic binding energies are not calculated in this paper.

The total valence-band Hamiltonian for a p-like multiplet under a strain field can be written as[12]

$$H_{tot} = H_{so} + H_1 + H_2 + H_{kin} , \tag{3}$$

where H_{kin} and H_{so} are the kinetic and the spin-orbit Hamiltonian, respectively. H_1 is the orbital-strain Hamiltonian, H_2 is the stress-dependent spin-orbit Hamiltonian. The expressions of H_1 and H_2 are given by

$$\begin{aligned} H_1 &= -a_1(e_{xx}+e_{yy}+e_{zz})L^2 - 3b_1[L_x^2 - L^2/3)e_{xx} + \text{c.p.}] - \sqrt{3}d_1[(L_xL_y + L_yL_x)e_{xy} + \text{c.p.}] , \\ H_2 &= -a_2(e_{xx}+e_{yy}+e_{zz})(L\sigma) - 3b_2[(L_x\sigma_x - L\sigma/3)e_{xx} + \text{c.p.}] - \sqrt{3}d_2[(L_x\sigma_y + L_y\sigma_x)e_{xy} + \text{c.p.}] , \end{aligned} \tag{4}$$

where L is the angular momentum operator, σ is the Pauli matrix vector, and c.p. denotes the cyclic permutation with respect to the indices x, y, and z. The quantities a_1, b_1, and d_1 (a_2, b_2, and d_2), are orbital (spin-dependent) deformation potentials.

For the case of (0,0,1)-oriented built-in stress, we keep the distribution of the 6×6 valence-band matrix as two equivalent 3×3 block-diagonal matrices of the following kind:

$$\begin{array}{ccc} |\phi_h\rangle & |\phi_l\rangle & |\phi_{so}\rangle \end{array}$$

$$\begin{bmatrix} -a(e_{xx}+e_{yy}+e_{zz}) - b(e_{zz}-e_{xx}) & 0 & 0 \\ 0 & -a(e_{xx}+e_{yy}+e_{zz}) + b(e_{zz}-e_{xx}) & -\sqrt{2}b'(e_{zz}-e_{xx}) \\ 0 & \sqrt{2}b'(e_{zz}-e_{xx}) & -a'(e_{xx}+e_{yy}+e_{zz}) \end{bmatrix} , \tag{5}$$

where e_{ij} are the components of the strain field, and the deformation potentials a, a', b, and b' are given by $a = a_1 + a_2$; $a' = a_1 - 2a_2$; $b = b_1 + 2b_2$; $b' = b_1 - b_2$.

To calculate the eigenstates in the valence band of our heterostructures, we have to ensure the continuity of both the envelope functions and probability current across the interfaces. A detailed description of the calculation of the in-plane dispersion relations of Γ_8-like confined states, *including the effect of coupled bands,* is given in Ref. 13.

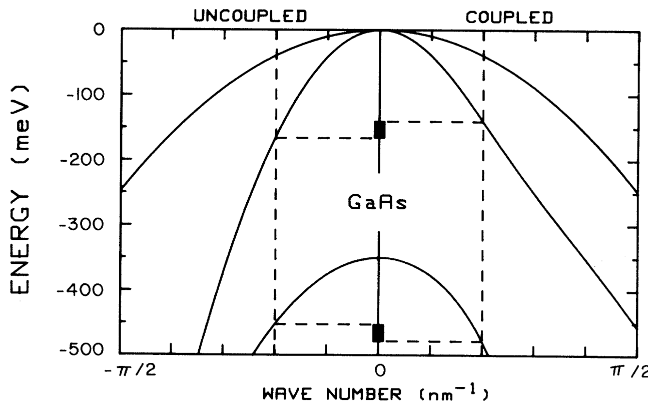

FIG. 3. Plot of the valence-band dispersion relations $E(k_z)$, for GaAs. On the left is the so-called "uncoupled" calculation (see text), for which the bands are parabolic. When the coupling between light and split-off states is taken into account ("coupled" situation), the corresponding bands become *nonparabolic,* as shown on the right-hand side of the figure. The solid rectangles represent the energy differences between both approximations, for the first quantized light and split-off levels, for the case of an infinitely deep, 5-nm-wide single quantum well. These differences are of the order of ~25 meV.

We assume a 33%–67% division of the gap difference between the strained heavy-hole and conduction-electron potential depths, which is known to be the correct partition for GaAs-AlAs microstructures.[14,15]

The result of this last calculation, made using the parameters of Refs. 6, 12, and 16–18, is illustrated in Fig. 2 (solid line). By comparison with the reflectance data, it is clear that the inclusion of the light-hole interaction with the split-off hole is sound and fundamental if we are to explain the experimental observations. A modest discrepancy still remains between the experimental data and the calculation. This we attribute to the difference between the Rydberg energies of light-hole excitons and heavy-hole excitons. No calculation of the Rydberg energies is available for the 6×6 full valence Hamiltonian: The off-diagonal term in Eq. (2) was omitted in all the earlier works on the subject. Most calculations were made at $k_x = k_y = 0$, and show that the light-hole exciton has a larger Rydberg than the heavy-hole one. More recent calculations, which include the contributions of states away from $k_x = k_y = 0$ and the mismatch of dielectric constants[19] demonstrate an enhancement of this difference. Qualitatively, this can be explained as follows: in the calculation of the Γ_8 Rydberg, a significant contribution to the difference between calculated values originates in the difference between the light-hole and heavy-hole in-plane masses. The light-hole (heavy-hole) excitons have a heavy (light) in-plane reduced mass, giving large (small) values of the Rydbergs. Andreani and Pasquarello[19] have estimated a difference between light-hole and heavy-hole excitons for GaAs-AlAs of 9 meV for a 3-nm well, and 6 meV for a 4-nm well. Assuming similar differences for our (Ga,In)As-AlAs samples with 3 and 3.8 nm brings the experimental points in excellent agreement with the calculated curve in Fig. 2 (solid line). The increasing energy

difference between experiment and theory, as the well width is reduced, is consistent with the trend proposed by Grundmann and Bimberg[20] in the narrow well range. Our results are consistent with the light-hole Rydberg remaining larger than the heavy-hole one, for this range of well widths.

In conclusion, we wish to emphasize the fact that a correct estimate of light-hole confinement energies in quantum wells requires the inclusion of the coupling with the split-off band when the light-hole potential depth is comparable to the value of the energy difference between Γ_8^v and Γ_7^v. This has been demonstrated experimentally for the case of (Ga,In)As-AlAs quantum wells with low indium concentration. Further investigations are required to quantify the influence of the light hole to split-off hole interactions. This may be particularly important, for instance, in predicting threshold currents for (Ga,In)As-GaAs strained-layer quantum-well lasers, for which interesting results have been predicted,[21] invoking valence-band physics. The results shown in this paper demonstrate unambiguously that device designers cannot restrict the valence-band physics to the Γ_8 states without care in their model calculations. This is particularly true for strained layers quantum wells and superlattices where the light-hole and split-off hole states are coupled by *both* the kinetic-energy Hamiltonian and the strain.

[1]For a review, see, for instance, *The Quantum Hall Effect: Graduate Text in Contemporary Physics,* edited by S. R. E. Prange and S. M. Girvin (Springer-Verlag, Berlin, 1987).

[2]P. Voisin, J. Bleuse, C. Bouche, S. Gaillard, C. Alibert, and A. Regreny, Phys. Rev. Lett. **61**, 1639 (1988); E. E. Mendez, F. Agullo-Rueda, and J. M. Hong, *ibid.* **60**, 2426 (1988).

[3]K. J. Moore, G. Duggan, G. Th. Jaarsma, P. F. Fewster, K. Woodbridge, and R. J. Nicholas, Phys. Rev. B **43**, 12393 (1991).

[4]J. W. Matthews and A. E. Blakeslee, J. Cryst. Growth **27**, 118 (1974).

[5]I. J. Fritz, S. T. Picraux, L. R. Dawson, T. J. Drummond, W. D. Laidig, and N. G. Anderson, Appl. Phys. Lett. **46**, 967 (1985).

[6]Geoffrey Duggan, Karen J. Moore, Bryce Samson, Age Raukema, and Karl Woodbridge, Phys. Rev. B **42**, 5142 (1990).

[7]M. F. H. Schuurmans, and G. W. t'Hooft, Phys. Rev. B **31**, 8041 (1985).

[8]R. Eppenga, M F. H. Schuurmans, and S. Colak, Phys. Rev. B **36**, 1554 (1987).

[9] P. Boring, B. Gil, P. Lefebvre, and K. J. Moore (unpublished).

[10]G. Ji, D. Huang, U. K. Reddy, T. S. Henderson, R. Houdre, and H. Morkoç, J. Appl. Phys. **62**, 3366 (1987).

[11]S. H. Pan, H. Shen, Z. Hang, F. H. Pollak, Weilma Zhuang, Qian Xu, A. P. Roth, R. A. Masut, C. Lacelle, and D. Morris, Phys. Rev. B **38**, 3375 (1988).

[12]M. Chandrasekhar and F. H. Pollak, Phys. Rev. B **15**, 2127 (1977).

[13]L. C. Andreani, A. Pasquarello, and F. Bassani, Phys. Rev. B **36**, 5887 (1987).

[14]G. Danan, B. Etienne, F. Mollot, R. Planel, A. M. Jean-Louis, F. Alexandre, B. Jusserand, G. Leroux, J. Y. Marzin, H. Savary, and B. Sermage, Phys. Rev. B **35**, 6207 (1987).

[15]K. J. Moore, P. Dawson, and C. T. Foxon, Phys. Rev. B **38**, 3368 (1988).

[16]K. J. Moore, G. Duggan, P. Dawson, and C. T. Foxon, Phys. Rev. B **38**, 5535 (1988).

[17]P. Lefebvre, B. Gil, H. Mathieu, and R. Planel, Phys. Rev. B **40**, 7802 (1989).

[18]K. J. Moore, G. Duggan, K. Woodbridge, and C. Roberts, Phys. Rev. B **41**, 1090 (1990).

[19]L. C. Andreani and A. Pasquarello, Phys. Rev. B **42**, 8928 (1990), and references therein.

[20]M. Grundmann and D. Bimberg, Phys. Rev. B **38**, 13486 (1988).

[21]D. Ahn and Shun-Lien Chuang, IEEE J. Quantum Electron. **24**, 2400 (1988).